

yellow oil. Trituration of this oil with hexanes for 0.5 h gave the product as a pale-yellow solid in >80% yield:  $^1\text{H NMR}$  ( $\text{C}_6\text{D}_6$ )  $\delta$  5.48 (s, 10 H,  $\text{Cp}_2\text{Zr}$ ), 2.22 (s, 3 H, acetyl methyl); IR (toluene) 1718, 1401, 1209, 1147, 1017, 812  $\text{cm}^{-1}$ .

**Complex 6: The  $\text{O}_2\text{CCF}_3^-$  Analogue of 4a.**  $\text{Cp}_2\text{ZrMe}_2$  (0.030 g, 0.12 mmol) and  $\text{Cp}_2\text{Zr}(\eta^2\text{-COMe})(\text{O}_2\text{CCF}_3)$  (0.055 g, 0.14 mmol) were sealed in an NMR tube as a  $\text{C}_6\text{D}_6$  solution. The solution turned yellow, and a pale-yellow crystalline precipitate was isolated by filtration after 1 h. The compound was thermally unstable, decomposing at room temperature in about a day:  $^1\text{H NMR}$  ( $\text{C}_6\text{D}_6$ )  $\delta$  5.84 (s, 10 H,  $\text{Cp}_2\text{Zr}$ ), 5.74 (s, 10 H,  $\text{Cp}_2\text{Zr}$ ), 1.48 (s, 6 H, acetone methyls), 0.49 (s, 3 H,  $\text{ZrMe}$ ); IR (toluene) 1709, 1205, 1181, 1138, 810  $\text{cm}^{-1}$ .

**Deprotonation of 2a with LDA at Low Temperature.** A double male (14/20) glass filtration frit, connected to a vacuum line with a horizontal 14/20 joint permitting the inversion of the frit, was fitted with a round-bottom flask on each end. A suspension of **2a** (0.100 g, 0.196 mmol) and LDA (0.021 g, 0.196 mmol) in  $\text{Et}_2\text{O}$  (10 mL) was stirred at  $-42^\circ\text{C}$  in one flask for 1 h. The suspension was then stripped of solvent and extracted with benzene and the benzene filtered to yield a tan precipitate and a yellow solution. The precipitate was found to be  $\text{Li}^+\text{-CpMo}(\text{CO})_3^-$  by comparison of its IR to that of an authentic sample independently synthesized from LDA and  $\text{HMo}(\text{CO})_3\text{Cp}$ . The solvent was removed to yield a pale-yellow oil, which upon titration with hexanes gave the product as a white powder. The product was shown by NMR to be the ketene complex **5** previously reported<sup>4</sup> from the deprotonations of  $\eta^2$ -acetyls.

**Reaction of 2a with MeLi at  $-80^\circ\text{C}$ .** Using the filtration apparatus described above, a yellow solution of **2a** (0.100 g, 0.19 mmol) in THF (5 mL) was cooled to  $-80^\circ\text{C}$  and allowed to stir for 0.5 h. To the cold stirring solution 1 equiv of MeLi was added dropwise. After 10 min, the flask was allowed to warm (0.5 h) to room temperature. The mixture was then stirred for an additional 0.5 h. The solution was reduced in volume, and addition of hexanes and filtration yielded a pale-yellow solid

( $\text{Li}^+\text{CpMo}(\text{CO})_3^-$ , identified by its IR). The filtrate was pumped to dryness, yielding an orange-yellow residue, shown by  $^1\text{H NMR}$  ( $\text{C}_6\text{D}_6$  and  $\text{CDCl}_3$ ) to be mostly the known<sup>4</sup> Zr ketene complex **5**.

**Complex 7: Reaction of 4a with CO.** A degassed solution of **4a** (0.102 g, 0.13 mmol) in toluene (3 mL) was pressurized with >1 atm of CO. The solution was then cooled in an ice bath and allowed to stir at  $0^\circ\text{C}$  for 4.5 h. The solvent was then removed in vacuo to yield a light-yellow powder. The powder was washed with 2 mL of a 80:20 mixture of hexanes and benzene to give the product in 55% yield:  $^1\text{H NMR}$  ( $\text{C}_6\text{D}_6$ )  $\delta$  5.76 (s, 10 H,  $\text{Cp}_2\text{Zr}$ ), 5.74 (s, 10 H,  $\text{Cp}_2\text{Zr}$ ), 5.39 (s, 5 H, CpMo), 1.01 (s, 6 H, acetone methyls), 0.25 (s, 3 H,  $\text{ZrMe}$ ); IR (toluene) 1931, 1840, 1591, 1180.6, 1017, 804  $\text{cm}^{-1}$ . Anal. Calcd for  $\text{C}_{32}\text{H}_{34}\text{O}_5\text{MoZr}_2$ : C, 50.23; H, 4.30. Found: C, 50.08; H, 4.40.

In a separate experiment, a calibrated vacuum bulb with **4a** (0.104 g, 0.137 mmol) in toluene (20 mL) was observed manometrically to take up CO (0.124 mmol, 0.91 equiv) at  $20^\circ\text{C}$  over the course of 3.25 h.

**Acknowledgment.** This research was partially supported by NSF Grant CHE82-07597. Acknowledgment is also made to the donors of the Petroleum Research Fund, administered by the American Chemical Society, for partial support of this work. We thank Prof. S. H. Strauss for assistance in the manometric measurements. The Nicolet R3m/E diffractometer and computing system at Colorado State University was purchased with funds provided by the National Science Foundation (Grant CHE-8103011).

**Supplementary Material Available:** Tables of all bond lengths and angles, anisotropic thermal parameters for non-hydrogen atoms, positional parameters of hydrogen atoms, and observed and calculated structure factors (31 pages). Ordering information is given on any current masthead page.

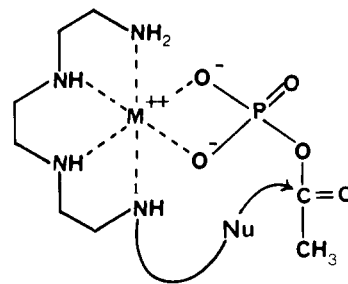
## Association Phenomena. 6. NMR Studies of the Mixed Chelates of Triethylenetetramine, Phosphate, and Metal Ions

George C. Mei and C. David Gutsche\*

Contribution from the Department of Chemistry, Washington University, St. Louis, Missouri 63130. Received February 27, 1985

**Abstract:** Experiments reported in earlier papers in this series described the synthesis of several polyamines and polyamides carrying pendant arms terminating in nucleophilic groups. These compounds were designed as catalysts for the decomposition of acetyl phosphate on the premise that the polyamines or polyamides would form mixed chelates with metal ions and acetyl phosphate and that the forced proximity of the nucleophile and acetyl moieties would lead to pseudointramolecular acyl transfer. The observed rates of catalyzed decomposition of acetyl phosphate, however, were far lower than anticipated. The reasons for this failure to observe catalysis are probed in the present work by using a model system consisting of triethylenetetramine, phosphate, and metal ions. By means of  $^{31}\text{P}$  NMR measurements of longitudinal and transverse relaxation rates, we show that mixed chelates containing the polyamine, metal ion, and phosphate do, indeed, form to a finite extent and that the entry and exit of the phosphate into and out of the complex occur sufficiently rapidly to preclude them as rate-determining steps in the acetyl phosphate decomposition reaction.

Two earlier papers of this series<sup>1,2</sup> described studies of the hydrolysis of acetyl phosphate. Lau and Gutsche<sup>2</sup> attempted to detect polyfunctional catalysis of the process by using various polyamines or polyamides and metal ions, the premise being that a mixed chelate (**1**) would form from the metal ion, the amine or amide, and acetyl phosphate and that its geometry would promote intramolecular displacement of the acetyl group by the nucleophilic moiety of the polyamine or polyamide. However, only modest rate enhancements were observed, and the purpose of the present paper is to explore some of the possible reasons for this behavior. In particular, the questions of the extent of mixed-chelate formation and the rate at which a phosphate moiety



1

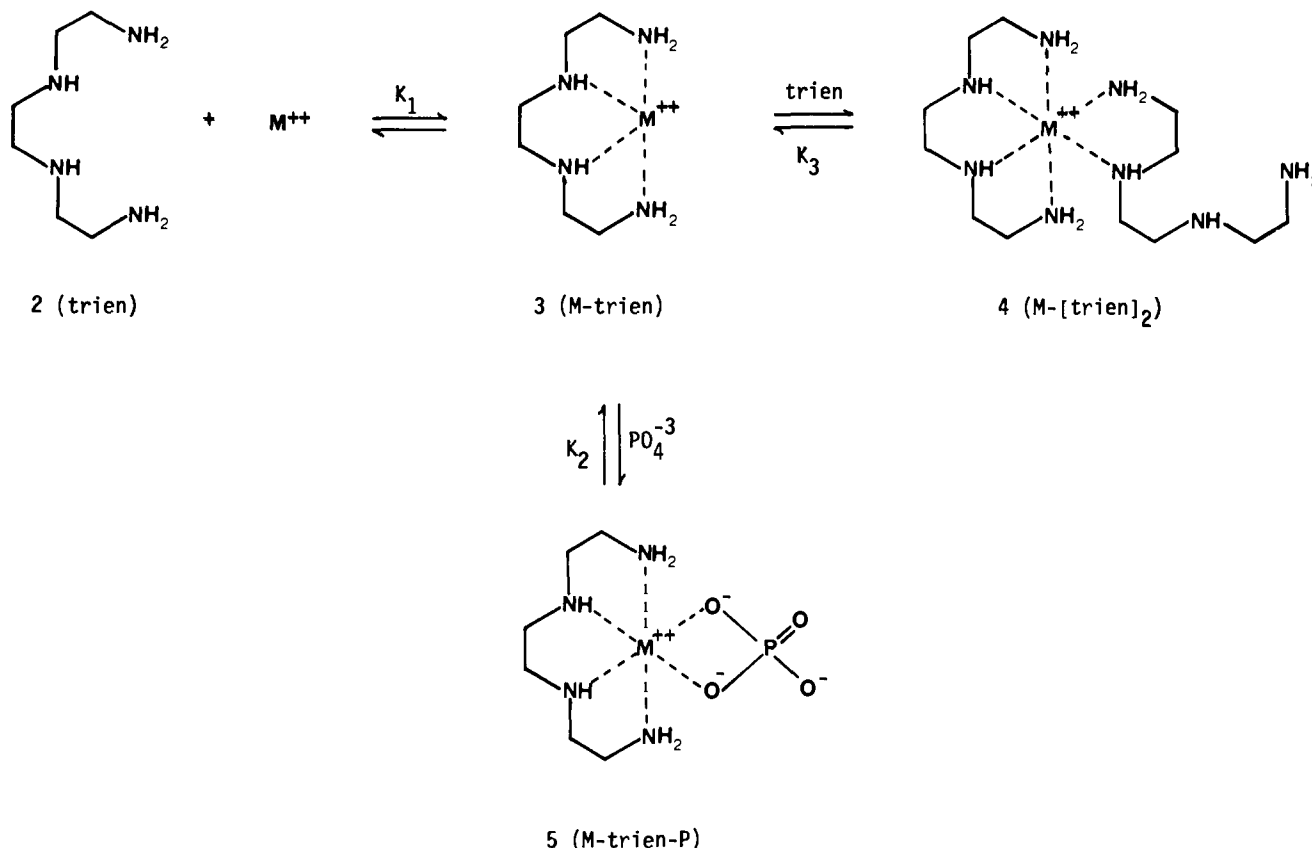
enters and leaves the mixed chelate are addressed.

The system chosen for study included triethylenetetramine (**2**)

(1) Melhado, L. L.; Gutsche, C. D. *J. Am. Chem. Soc.* **1978**, *100*, 1850.

(2) Lau, H.-p.; Gutsche, C. D. *J. Am. Chem. Soc.* **1978**, *100*, 1857.

Scheme I



(trien) as the polyamine, inorganic phosphate, and the metal ions<sup>3</sup> Cu<sup>2+</sup>, Ni<sup>2+</sup>, Mn<sup>2+</sup>, and Fe<sup>3+</sup>. <sup>31</sup>P NMR was considered to be the best probe, making use of measurements of the longitudinal relaxation times ( $T_1$ ) and transverse relaxation times ( $T_2$ ). The paramagnetic metal ions greatly reduce the transverse relaxation times and allow relatively low concentrations of the metal ions to be used. Since paramagnetic relaxation is the dominant mechanism in most instances, other relaxation effects can be ignored and simpler mathematical analyses can be employed.

**Stability Constants of Mixed Metal Chelates via the Measurement of Longitudinal Relaxation Rates.** The observed longitudinal relaxation rate ( $R_{\text{obsd}}$ ) for the system being studied is the sum of the relaxation rate of the free phosphate ( $R_0$ ) multiplied by the fraction of free phosphate ( $1 - P_m$ ) and the relaxation rate of the bound phosphate ( $R_m$ ) multiplied by the fraction of the bound phosphate ( $P_m$ ),

$$R_{\text{obsd}} = R_0(1 - P_m) + R_m P_m \quad (1)$$

When the total metal ion concentration ( $[M]_0$ ) is low compared to the total trien concentration ( $[\text{trien}]$ ) as well as the total phosphate concentration ( $[P]_0$ ), it can be assumed that essentially all the metal ions are complexed in one form or another and that the free trien and free phosphate concentrations are approximately equal to their total concentrations, i.e.,  $[M]_0 \approx [M\text{-trien}] + [M\text{-trien-P}]$ ,  $[\text{trien}] \approx [\text{trien}]_0$ , and  $[P] \approx [P]_0$ . Expression 1, accordingly, can be simplified to

$$R_{\text{obsd}} = R_0 + R_m P_m = R_0 + \frac{R_m [M\text{-trien-P}]}{[P]_0} \quad (2)$$

and the equilibrium constant,  $K = [M\text{-trien-P}]/[M\text{-trien}][P]$ , can be simplified and rearranged to

$$[M\text{-trien-P}] = \frac{[P]_0 [M]_0}{1 + K[P]_0} \quad (3)$$

The "excess" rate ( $R_e$ ), defined as the difference between  $R_{\text{obsd}}$  and  $R_0$ , is determined only by the paramagnetic relaxation mechanism.

$$R_e = R_{\text{obsd}} - R_0 = \frac{R_m [M\text{-trien-P}]}{[P]_0} \quad (4)$$

Combining expressions 3 and 4 gives an expression in which  $R_e$  is proportional to the total metal ion concentration;

$$R_e = \frac{R_m K [M]_0}{1 + K[P]_0} = \alpha [M]_0 \quad (5)$$

A plot of  $R_e$  vs.  $[M]_0$  gives a straight line with the slope defined as

$$\alpha = \frac{R_m K}{1 + K[P]_0} \quad (6)$$

Taking the reciprocal of expression 6, a plot of  $1/\alpha$  vs.  $[P]$  gives a straight line from which the values of  $R_m$  and  $K$  can be calculated from the slope and intercept, respectively.

$$\frac{1}{\alpha} = \frac{1}{R_m K} + \frac{[P]_0}{R_m} \quad (7)$$

Thus, the experiments involved first the measurement of  $R_e$  as a function of metal ion concentration at a given phosphate ion concentration, as illustrated in Figure 1 for Cu<sup>2+</sup>. Then, using the values of the slopes obtained from a series of such measurements at various phosphate ion concentrations, application of expression 7 produced values for  $R_m$  and  $K$ , as illustrated in Figure 2 for Cu<sup>2+</sup>.

(3) Co<sup>2+</sup> was included in the group of metals to be investigated, but relaxation rates could not be obtained for this ion because of the very rapid oxidation to Co<sup>3+</sup> during the course of the measurements. Even with carefully degassed samples, the rate of oxidation was rapid enough to obscure the results.

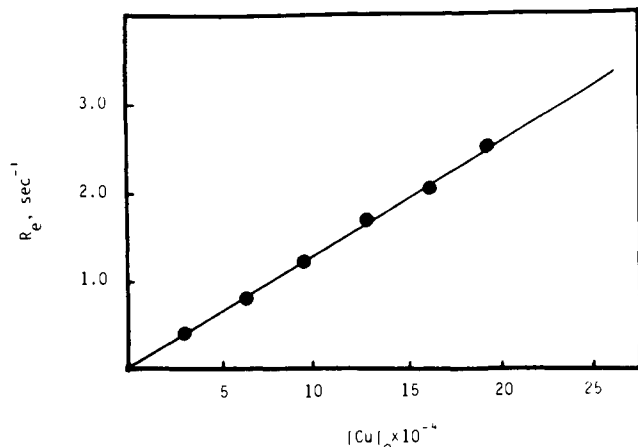


Figure 1. Relationship between  $R_e$  and  $\text{Cu}^{2+}$  at  $[\text{P}]_0 = 0.333 \text{ M}$ ,  $[\text{trien}]_0 = 0.326 \text{ M}$ , and  $\text{pH} 11.6$ .

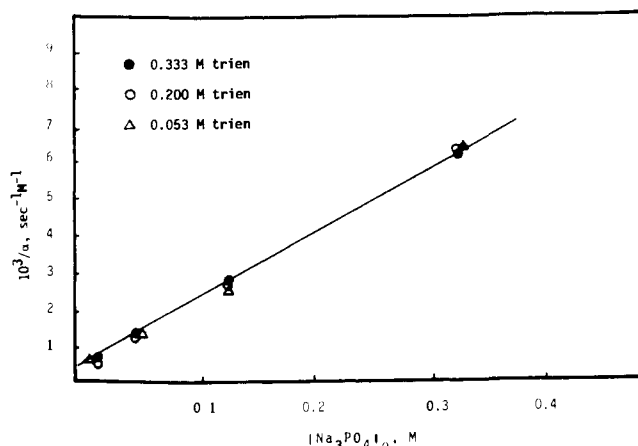


Figure 2. Effect of  $[\text{P}]_0$  and  $[\text{trien}]_0$  on  $\alpha$  (see expression 6) at  $25^\circ\text{C}$  and  $\text{pH} 11.6$  on a system containing  $\text{Cu}^{2+}$ .

In the event that competition between trien and phosphate plays a role in the system, a slight modification of expression 5 must be made. In addition to the equilibrium constant ( $K$ ) between metal-trien and metal-trien-phosphate, another equilibrium constant ( $K'$ ) for the competing processes needs to be defined as

$$K' = \frac{[\text{M}-(\text{trien})_2]}{[\text{M}-\text{trien}][\text{trien}]} = \frac{[\text{M}-(\text{trien})_2]}{[\text{M}-\text{trien}][\text{trien}]_0} \quad (8)$$

Expression 5 then becomes

$$R_e = \frac{R_m K [\text{M}]_0}{1 + K[\text{P}]_0 + K'[\text{trien}]_0} = \alpha' [\text{M}]_0 \quad (9)$$

and the slope  $\alpha'$  is expressed as

$$\alpha' = \frac{[\text{P}]_0}{R_m} + \frac{1}{K_{\text{eff}} R_m} \quad (10)$$

where  $1/K_{\text{eff}} = 1/K + K'[\text{trien}]/K$ . Only in the case of  $\text{Fe}^{3+}$ , however, was this of any consequence, where it accounted for only about 5% of the total effect. A plot of  $1/K_{\text{eff}}$  vs.  $[\text{trien}]$  for the  $\text{Fe}^{3+}$ -trien-phosphate system is shown in Figure 3.

When the method described above was used, the stability constants were determined for  $\text{Cu}^{2+}$ ,  $\text{Ni}^{2+}$ ,  $\text{Mn}^{2+}$ , and  $\text{Fe}^{3+}$ , as shown in Table I.

**Exchange Rates of Mixed Metal Chelates via the Measurement of Transverse Relaxation Rates.** A rigorous treatment of nuclear relaxation phenomena in solutions containing paramagnetic species and involving multisite exchange was developed by Swift and Connick<sup>4</sup> and later modified by Luz and Meiboom and others.<sup>5</sup>

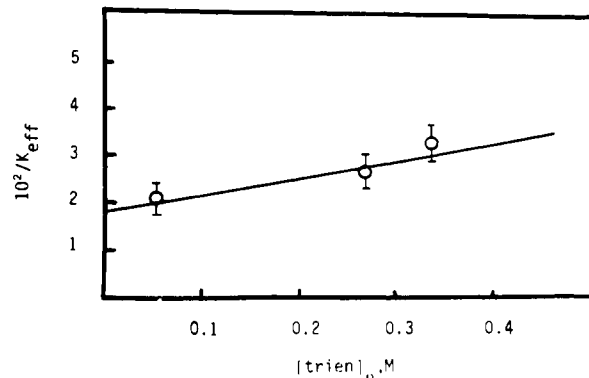


Figure 3. Effect of  $[\text{trien}]_0$  on the equilibrium between  $\text{Fe}^{3+}$ , trien, and phosphate.

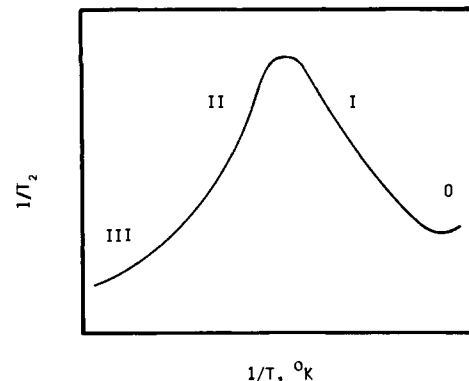


Figure 4. Schematic representation of the temperature dependence of the relaxation rates for a system undergoing chemical exchange.

Table I. Relaxation Rates and Stability Constants for Mixed Metal Chelates at  $25^\circ\text{C}$  and  $\text{pH} 11.6$

metal ion	$[\text{trien}]_0$	$R_m, \text{s}^{-1}$	$K, \text{M}^{-1}$	$K', \text{M}^{-1}$
$\text{Cu}^{2+}$	0.333	$54 \pm 1$	$81 \pm 10$	
$\text{Ni}^{2+}$	0.333	$360 \pm 4$	$26 \pm 4$	
	2.00	$420 \pm 5$	$25 \pm 4$	
$\text{Fe}^{3+}$	0.053	$1400 \pm 20$	$26 \pm 4$	
$\text{Fe}^{3+}$	0.333	$1600 \pm 27$	$61 \pm 9$	$3 \pm 1$
$\text{Mn}^{2+}$	0.333	$3800 \pm 35$	$120 \pm 13$	

Table II. Thermodynamic and Kinetic Data for Metal Mixed Chelates

metal ion	$\Delta H^\ddagger, \text{kcal/mol}$	$\Delta S^\ddagger, \text{cal/K/mol}$	$k, 10^3 \text{s}^{-1}$
$\text{Cu}^{2+}$	2.31	-30	$15.2 \pm 0.3$
$\text{Ni}^{2+}$	11.3	-3.7	$5.0 \pm 0.2$
$\text{Fe}^{3+}$	4.3	-17	$35.0 \pm 0.4$
$\text{Mn}^{2+}$	15.6	11	$2.8 \pm 0.1$

For solutions containing only one type of paramagnetic ion, the observed relaxation time ( $T_{2,\text{obsd}}$ ) is

$$\frac{1}{T_{2,\text{obsd}}} = \frac{1}{T_{2,0}} + \frac{P_m}{\tau_m} \left[ \frac{\frac{1}{T_{2,m}^2} + \frac{1}{\tau_m T_{2,m}} + \Delta\omega_m^2}{\left(\frac{1}{T_{2,m}} + \frac{1}{\tau_m}\right)^2 + \Delta\omega_m^2} \right] \quad (11)$$

where  $T_{2,\text{obsd}}$  and  $T_{2,0}$  are the transverse relaxation times for nuclei in solution in the presence and absence of paramagnetic species,  $T_{2,m}$  is the relaxation time in the metal complex,  $\tau_m$  is the average residence time of the nuclei in the metal coordination sphere

(4) Swift, T. J.; Connick, R. E. *J. Chem. Phys.* **1962**, *37*, 307.

(5) Luz, Z.; Meiboom, S. *J. Chem. Phys.* **1964**, *40*, 1058, 2686. Murray, R.; Dodgen, H. W.; Hunt, J. P. *Inorg. Chem.* **1964**, *3*, 1576. Glaeser, H. H.; Dodgen, H. W.; Hunt, J. P. *Ibid.* **1965**, *4*, 1061.

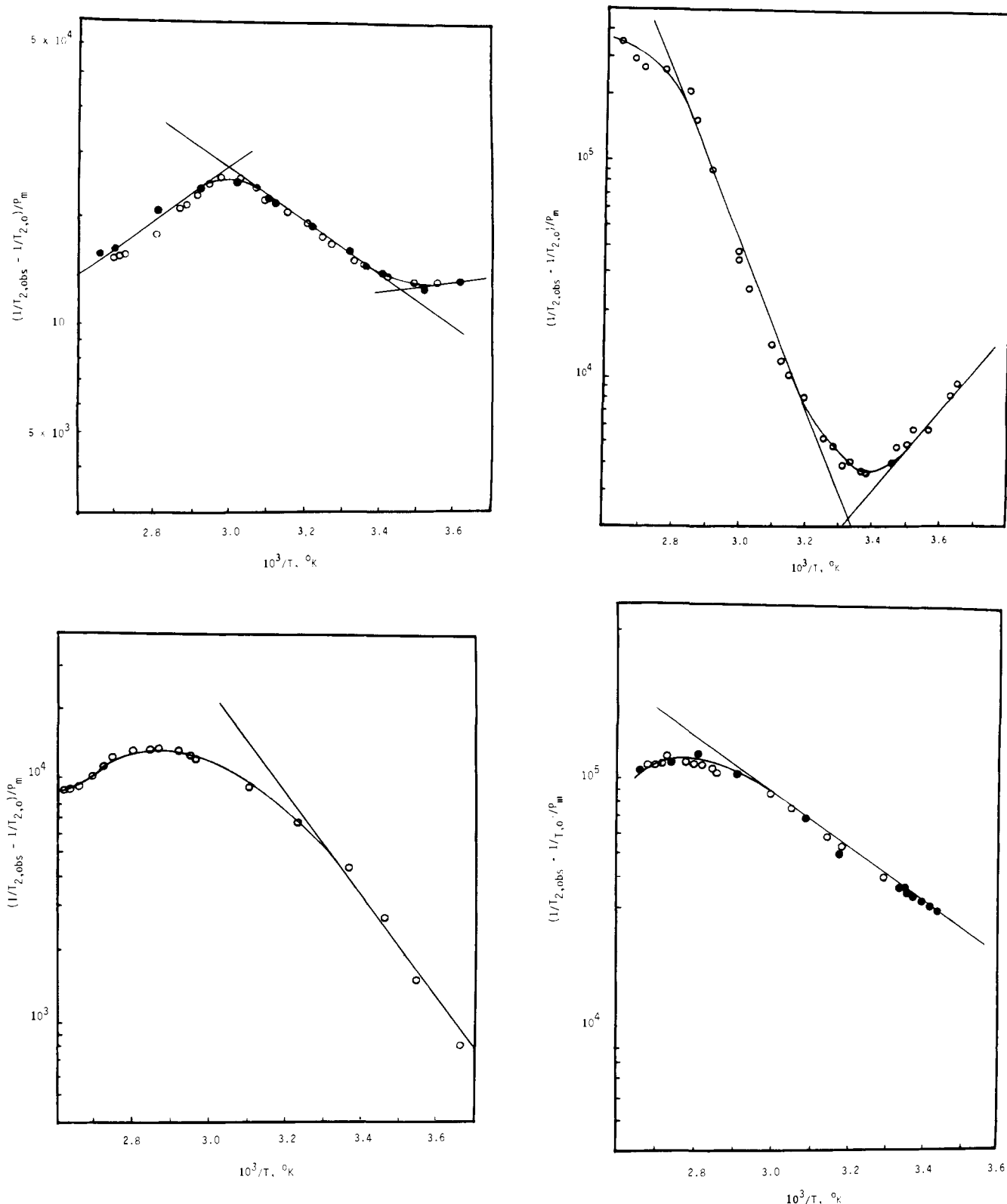


**Figure 5.**  $^{31}\text{P}$  relaxation rates of phosphate in solution containing 0.333 M trien, 0.326 M phosphate, and a metal ion as a function of reciprocal temperature. (A, top left)  $[\text{Cu}^{2+}] = 1.73 \times 10^{-3}$  M. (B, top right)  $[\text{Ni}^{2+}] = 2.12 \times 10^{-3}$  M. (C, bottom left)  $[\text{Mn}^{2+}] = 3.62 \times 10^{-4}$  M. (D, bottom right)  $[\text{Fe}^{3+}] = 3.69 \times 10^{-4}$  M.

(coordination number  $n$ ),  $P_m$  is the mole fraction of nuclei bound to the paramagnetic metal ( $P_m = \tau_m/\tau_A$ ),  $\tau_A$  is the average lifetime of nuclei in the bulk solvent, and  $\Delta\omega_m$  is the chemical shift difference between the bound and unbound nuclei. The temperature dependence of the quantity  $1/T_{2,\text{obsd}}$  is illustrated in Figure 4 which shows a plot that can be divided into four regions, designated as 0, I, II, and III. In region 0, dipole-dipole interaction is the

dominant relaxation mechanism, and the longitudinal and transverse relaxation times are equal. Region I is characterized by "slow exchange" in which  $\Delta\omega_m^2 \gg 1/T_{2,m}^2$  and  $1/\tau_m^2$  simplifying expression 11 to

$$\frac{1}{T_{2,\text{obsd}}} = \frac{1}{T_{2,0}} + \frac{P_m}{\tau_m} \quad (12)$$

**Table III.** Values of  $\alpha$  (Expression 6) for  $\text{Ni}^{2+}$ ,  $\text{Cu}^{2+}$ ,  $\text{Fe}^{3+}$ , and  $\text{Mn}^{2+}$  at Various Concentrations of Triethylenetetramine and Phosphate at 25 °C and pH 11.6

[ $\text{Na}_3\text{PO}_4$ ] <sub>0</sub> , M	[trien] <sub>0</sub> , M	slope ( $\alpha$ ), $10^{-4} \text{ s}^{-1} \text{ M}^{-1}$			
		$\text{Ni}^{2+}$	$\text{Cu}^{2+}$	$\text{Fe}^{3+}$	$\text{Mn}^{2+}$
0.326	0.333	0.979 ± 0.017	0.162 ± 0.008	4.32 ± 0.06	1.12 ± 0.01
0.130	0.333	2.18 ± 0.036	0.367 ± 0.006	9.50 ± 0.14	2.58 ± 0.03
0.052	0.333	4.11 ± 0.06	0.861 ± 0.014	18.63 ± 0.26	6.67 ± 0.09
0.021	0.333	5.51 ± 0.11	1.52 ± 0.02		10.10 ± 0.15
0.326	0.200	1.71 ± 0.02	0.159 ± 0.002	4.55 ± 0.06	1.14 ± 0.01
0.130	0.200	2.41 ± 0.03	0.385 ± 0.005	10.53 ± 0.30	2.50 ± 0.05
0.052	0.200	4.65 ± 0.08	0.714 ± 0.012	22.20 ± 0.31	5.56 ± 0.08
0.021	0.200	7.41 ± 0.11	2.22 ± 0.02	33.30 ± 0.52	20.00 ± 0.13
0.326	0.053	3.92 ± 0.06	0.154 ± 0.002	4.70 ± 0.06	1.46 ± 0.01
0.130	0.053	8.55 ± 0.10	0.401 ± 0.006	11.29 ± 0.16	2.98 ± 0.03
0.052	0.053	15.85 ± 0.22	0.798 ± 0.012	21.19 ± 0.30	6.56 ± 0.08
0.021	0.053	22.77 ± 0.31	1.59 ± 0.02	42.48 ± 0.60	14.42 ± 0.23

By subtracting the outer-sphere contribution, obtained from extrapolation of region 0,  $1/\tau_m$  can be obtained from expression 11. Then, by plotting  $\log 1/P_m(1/T_{2,\text{obsd}} - 1/T_{2,0})$  vs.  $1/T$ , the enthalpy of activation ( $\Delta H^\ddagger$ ) can be obtained from the slope and the entropy of activation ( $\Delta S^\ddagger$ ) from the intercept, assuming the validity of expression 13.

$$\frac{1}{\tau_m} = \frac{kT}{h} e^{-\Delta H^\ddagger/RT} e^{\Delta S^\ddagger/R} \quad (13)$$

In region II, an increase in temperature leads to "exchange" narrowing, where  $T_{2,\text{obsd}}$  is determined by the change in precessional frequency (chemical shift  $\Delta\omega_m$ ), and in the limit of  $1/\tau_m^2 \gg \Delta\omega_m^2 \gg (\tau_m T_{2,m})^{-1}$

$$\frac{1}{T_{2,\text{obsd}}} = \frac{1}{T_{2,0}} + \tau_m \Delta\omega_m^2 P_m \quad (14)$$

Region III is characterized by "fast exchange" where the measured relaxation rate is essentially the weighted average of the two environments, i.e.,  $(T_{2,m}\tau_m)^{-1} \gg 1/T_{2,m}$  and  $\Delta\omega^2$ , leading to

$$\frac{1}{T_{2,\text{obsd}}} - \frac{1}{T_{2,0}} = \frac{P_m}{T_{2,m}} \quad (15)$$

Plots of  $(1/T_{2,\text{obsd}} - 1/T_{2,0})/P_m$  vs.  $1/T$  for the four paramagnetic ions studied are shown in Figure 5. The values for  $P_m$  were calculated from the stability constants and in all cases were close to the ratio  $[M]_0/[P]_0$ . Region I is observed for all four ions, region II is observed for  $\text{Cu}^{2+}$ , and region 0 is observed for  $\text{Cu}^{2+}$  and  $\text{Mn}^{2+}$ . The thermodynamic data calculated from expressions 12 and 13 are shown in Table II. Although the  $\Delta G^\ddagger$  values remain fairly constant throughout the series of ions, there is considerable variation in the  $\Delta H^\ddagger$  and  $\Delta S^\ddagger$  values. It is uncertain whether this has a rational explanation or is simply the result of experimental error.

**Discussion.** The failure of Lau and Gutsche<sup>2</sup> to observe appreciable rate enhancements for the decomposition of acetyl phosphate in the presence of polyamines and metals can be ascribed to a number of factors. Most obvious among these is the question of whether metal mixed chelates such as structure **1** actually exist. The present data provide evidence that indeed they do exist but that the equilibrium constants for association are fairly modest. If it is assumed that acetyl phosphate and  $\text{PO}_4^{3-}$  form the mixed chelate to a similar extent, it can be calculated from the data in Table I that under the conditions used in the Lau and Melhado experiments, the amount of phosphate bound was ca. 40% for  $\text{Cu}^{2+}$ , 19% for  $\text{Ni}^{2+}$ , 48% for  $\text{Fe}^{3+}$ , and 34% for  $\text{Mn}^{2+}$ . This degree of association should be sufficient for demonstrable catalysis: (a) if the other necessary features such as appropriate stereochemistry and sufficient intramolecular nucleophilicity are met *and* (b) if the metal mixed chelate exists for a long enough time for reaction to occur. That the lifetime of the complex is

not the limiting feature in these systems is indicated by the data in Table II which show that it is on the order of  $10^{-4}$  s, a time sufficiently long for as many as  $10^6$  collisions to occur. Although the present data do not answer the question of why the Lau and Gutsche system fails to yield significant rate enhancements, they do give encouragement to the possibility of using a metal mixed chelate as a means for achieving polyfunctional catalysis.

### Experimental Section

**Measurement of Longitudinal ( $T_1$ ) and Transverse ( $T_2$ ) Relaxation Times.** A 2.00-mL sample of a stock solution of trien and phosphate was transferred to a 10-mm NMR tube by means of a 10-mL pipet, and the NMR tube was then tightly capped with a septum. Inserted through the septum was a needle attached to a system that allowed vacuum and nitrogen to be alternately applied. During the time that the NMR tube was being evacuated, it was shaken on a vibrator, bubbles emerging in copious amount. When the bubbling subsided, the tube was filled with nitrogen, and this cycle was repeated several times to ensure complete removal of oxygen from the samples. In a separate tube, a stock solution of the metal ion was degassed in a similar fashion, and immediately before the measurements were made, 30–180  $\mu\text{L}$  of this solution were added by injection through the septum of the NMR tube containing the trien and phosphate. The metal ion concentration was adjusted so that  $T_1$  was about 0.5 s; too large a  $T_1$  makes the nuclear relaxation time too long, and too small a  $T_1$  broadens the resonances and reduces the accuracy. The  $T_1$  and  $T_2$  measurements were made on a JEOL FX-100 FT spectrometer, pulses were generated by a Rockland Model 5610A frequency synthesizer, and the relaxation data were calculated with a Texas Instrument Model 980 computer. A gas flow cryostat (NMR 5471 VT controller) provided with heated or cooled air was used to regulate the temperature of the solutions, and the temperatures were calibrated with an OMEGA 2160A digital thermometer to an accuracy of 1 °C. The  $T_1$  values were obtained by a 180–90° pulse sequence (inverse recovery method), and the  $T_2$  values were obtained by a 90°/180° (90° phase shift) pulse sequence (Carr, Purcell, Meiboom, Gill method). The  $\alpha$  values (expression 6) obtained from  $T_1$  measurements are shown in Table III for  $\text{Ni}^{2+}$ ,  $\text{Cu}^{2+}$ ,  $\text{Fe}^{3+}$ , and  $\text{Mn}^{2+}$ .

**Stock Solutions.** Triethylenetetramine (Aldrich) was distilled under vacuum and obtained as a clear, colorless liquid. Manganese chloride, nickel chloride, cupric chloride, ferric chloride, and cobalt chloride (Mallinckrodt analytical grade chemicals) were used without further purification. The distilled water was boiled for 30 min to expell carbon dioxide, cooled, and stored in a plastic bottle. Stock solutions of phosphate and trien were prepared by dissolving the appropriate amounts of  $\text{Na}_3\text{PO}_4 \cdot 12\text{H}_2\text{O}$  (to give concentrations ranging from 0.029 to 0.326 M) and triethylenetetramine (to give concentrations ranging from 0.0527 to 0.333 M) in distilled water in a 500-mL glass-stoppered volumetric flask. Stock solutions of the metal ions were prepared by dissolving the appropriate amounts of the metal chlorides (to give concentrations of approximately  $10^{-2}$  M) in a 1000-mL glass-stoppered volumetric flask.

**Acknowledgment.** This work was supported, in part, by a National Institutes of Health grant and a Biomedical Science Support grant. We are especially indebted to Prof. Joseph J. H. Ackerman for this invaluable help in the obtention and interpretation of the nuclear magnetic resonance data.